

A New 25-Metal-Atom Supracluster: Synthesis, Characterization, and Crystal Structure of the Ternary Cluster Compound $[\text{Pt}_2(\text{AuPPh}_3)_{10}\text{Ag}_{13}\text{Cl}_7]$

T. G. M. M. Kappen, P. P. J. Schlebos, J. J. Bour, W. P. Bosman, J. M. M. Smits, P. T. Beurskens, and J. J. Steggerda*

Department of Inorganic Chemistry and Crystallography, Faculty of Science, University of Nijmegen, Toernooiveld, 6525 ED Nijmegen, The Netherlands

Received June 29, 1993*

A new neutral Pt–Au–Ag cluster compound is reported: $[\text{Pt}_2(\text{AuPPh}_3)_{10}\text{Ag}_{13}\text{Cl}_7]$. This 25-metal-atom supracluster is formed by the reaction of $[\text{Pt}(\text{H})(\text{PPh}_3)(\text{AuPPh}_3)_7](\text{NO}_3)_2$ with $\text{Ag}(\text{PPh}_3)(\text{NO}_3)$ in a molar ratio of 1:4 with subsequent addition of NaCl. This compound was characterized by elemental analysis, IR and ^{31}P NMR spectroscopy, FAB-MS, and cyclic voltammetry. The crystal and molecular structure of $[\text{Pt}_2(\text{AuPPh}_3)_{10}\text{Ag}_{13}\text{Cl}_7]$ has been determined by a single-crystal X-ray analysis. The compound crystallizes with about 10 solvent molecules in the monoclinic space group $P2_1/m$, with $a = 17.154(2)$ Å, $b = 25.256(2)$ Å, $c = 29.889(2)$ Å, $\beta = 106.13(2)^\circ$, $V = 12439$ Å³, and $Z = 2$. Mo $K\alpha$ radiation was used. The residuals are $R = 0.089$ and $R_w = 0.084$ for 3585 observed reflections and 352 variables. The structure consists of two identical icosahedral Pt-centered subunits sharing a single common vertex, which is a silver atom. The central platinum atoms are bound to five gold atoms and seven silver atoms. A triphenylphosphine is attached to each of the gold atoms. The central silver atom is bound to ten silver atoms and two platinum atoms. The peripheral silver atoms are attached to terminal or μ^2 -bridging Cl ligands.

Introduction

Recently there has been substantial interest in high-nuclearity metal cluster compounds. The metal atoms in such clusters are often arranged in close-packed geometries resembling fragments of metallic lattices. Because the compositions and geometries of these clusters are often well-defined, they are of particular interest to small metal-particle physics and chemistry including catalysis.¹

A large number of mixed metal–gold clusters are known in which one to twelve gold atoms are attached to a central metal atom.^{2–5} Icosahedral-based geometries are often found for these types of cluster compounds. Whereas the variety of the central atom is extensive, only a limited number of other metals could be introduced into the periphery next to the gold atoms; e.g., mercury,⁶ tin,⁷ copper,⁸ and silver^{9,10} have been successfully incorporated into these mixed metal–gold cluster compounds.

Efforts to introduce silver into the well-characterized mixed platinum–gold cluster $[\text{Pt}(\text{H})(\text{PPh}_3)(\text{AuPPh}_3)_7]^{2+11}$ provided us with the new neutral cluster compound $[\text{Pt}_2(\text{AuPPh}_3)_{10}\text{Ag}_{13}\text{Cl}_7]$. This ternary Pt–Au–Ag cluster, with a relatively high silver to metal ratio, is a new member to the family of binary Au–Ag supraclusters formed by the reduction of mixtures of Au(I) and Ag(I) species in the presence of phosphines and described by Teo et al.^{12–14} However, this new Pt–Au–Ag supracluster has not been synthesized from such mononuclear building blocks but from the above-mentioned multinuclear PtAu_7 cluster. Therefore, this route of synthesis can be seen as further support of the “cluster of clusters” concept¹⁵ concerning this kind of supraclusters. Samples of about 25 mg could be prepared, so the compound could be characterized by elemental analysis and spectroscopic measurements.

In this paper we report the synthesis of $[\text{Pt}_2(\text{AuPPh}_3)_{10}\text{Ag}_{13}\text{Cl}_7]$ and its characterization by elemental analysis and FAB-MS, together with the spectroscopic data and crystal structure of this new ternary supracluster.

Experimental Section

Measurements. Elemental analyses were carried out at the Microanalytical Department of the University of Nijmegen. Fast atomic bombardment mass spectroscopy (FAB-MS) was executed on a VG Analytical Ltd. 7070E-HF mass spectrometer of the Mass Spectrometry Service Laboratory of the University of Minnesota. CsI was used as the

* Abstract published in *Advance ACS Abstracts*, January 1, 1994.

- (1) Aubart, M. A.; Pignolet, L. H. *J. Am. Chem. Soc.* **1992**, *114*, 7901.
- (2) Jennings, M. C.; Puddephatt, R. J.; Manojlović-Muir, L. J.; Muir, K. W.; Mwariri, B. N. *Organometallics* **1992**, *11*, 4164.
- (3) Richmond, M. G. *J. Organomet. Chem.* **1992**, *432*, 215.
- (4) Ragaini, F.; Cenini, S.; Fumagalli, A.; Crotti, C. *J. Organomet. Chem.* **1992**, *428*, 401.
- (5) Garland, M. *Organometallics* **1993**, *12*, 535.
- (6) Kappen, T. G. M. M.; van den Broek, A. C. M.; Schlebos, P. P. J.; Bour, J. J.; Bosman, W. P.; Smits, J. M. M.; Beurskens, P. T.; Steggerda, J. J. *Inorg. Chem.* **1992**, *31*, 4075.
- (7) Muetting, A. M.; Bos, W.; Alexander, B. D.; Boyle, P. D.; Casalnuovo, J. A.; Balaban, S.; Ito, L. N.; Johnson, S. M.; Pignolet, L. H. *New J. Chem.* **1988**, *12*, 505.
- (8) Braunstein, P.; Lehner, H.; Matt, D.; Tiripicchio, A.; Tiripicchio-Camellini, M. *Angew. Chem., Int. Ed. Engl.* **1984**, *23*, 304.
- (9) Bott, S. G.; Mingos, D. M. P.; Watson, M. J. *J. Chem. Soc., Chem. Commun.* **1989**, 1192.
- (10) Steggerda, J. J.; Bour, J. J.; van der Velden, J. W. A. *Recl. Trav. Chim. Pays-Bas* **1982**, *101*, 164.
- (11) Schoondergang, M. F. J.; Bour, J. J.; van Strijdonck, G. P. F.; Schlebos, P. P. J.; Bosman, W. P.; Smits, J. M. M.; Beurskens, P. T.; Steggerda, J. J. *Inorg. Chem.* **1991**, *30*, 2048.
- (12) Briant, C. E.; Theobald, B. R. C.; White, J. W.; Bell, L. K.; Mingos, D. M. P.; Welch, A. J. *J. Chem. Soc., Chem. Commun.* **1981**, 201.
- (13) van der Velden, J. W. A.; Vollenbroek, F. A.; Bour, J. J.; Beurskens, P. T.; Smits, J. M. M.; Bosman, W. P. *Recl. Trav. Chim. Pays-Bas* **1981**, *100*, 148.
- (14) Bour, J. J.; van den Berg, W.; Schlebos, P. P. J.; Kanters, R. P. F.; Schoondergang, M. F. J.; Bosman, W. P.; Smits, J. M. M.; Beurskens, P. T.; Steggerda, J. J.; van der Sluis, P. *Inorg. Chem.* **1990**, *29*, 2971.
- (15) Demidowicz, Z.; Johnston, R.; Mingos, D. M. P.; Williams, I. D. *J. Chem. Soc., Dalton Trans.* **1988**, 1751.
- (16) Mingos, D. M. P.; Powell, H. R.; Stonberg, T. L. *Transition Met. Chem. (London)* **1992**, *17*, 334.

- (8) Schoondergang, M. F. J.; Bour, J. J.; Schlebos, P. P. J.; Vermeer, A. W. P.; Bosman, W. P.; Smits, J. M. M.; Beurskens, P. T.; Steggerda, J. J. *Inorg. Chem.* **1991**, *30*, 4704.

- (9) Kanters, R. P. F.; Schlebos, P. P. J.; Bour, J. J.; Bosman, W. P.; Smits, J. M. M.; Beurskens, P. T.; Steggerda, J. J. *Inorg. Chem.* **1990**, *29*, 324.
- (10) Copley, R. C. B.; Mingos, D. M. P. *J. Chem. Soc., Dalton Trans.* **1992**, 1755.
- (11) Kanters, R. P. F.; Bour, J. J.; Schlebos, P. P. J.; Bosman, W. P.; Behm, H.; Steggerda, J. J.; Ito, L. N.; Pignolet, L. H. *Inorg. Chem.* **1989**, *28*, 2591.
- (12) Teo, B. K.; Shi, X.; Zhang, H. *J. Am. Chem. Soc.* **1991**, *113*, 4329.
- (13) Teo, B. K.; Zhang, H. *Inorg. Chem.* **1991**, *30*, 3115.
- (14) Teo, B. K.; Shi, X.; Zhang, H. *J. Chem. Soc., Chem. Commun.* **1992**, 1195.
- (15) Teo, B. K.; Zhang, H. *Polyhedron* **1990**, *9*, 1985.
- (16) Teo, B. K.; Zhang, H. *Inorg. Chim. Acta* **1988**, *144*, 173.
- (17) Teo, B. K.; Zhang, H.; Shi, X. *J. Am. Chem. Soc.* **1990**, *112*, 8552.

mass-calibration standard for the FAB-MS spectra, which were taken in a *m*-nitrobenzyl alcohol matrix. Further details of the experimental procedure can be found elsewhere.¹⁶

³¹P{¹H} NMR spectra of toluene solutions of the sample were recorded on a Bruker WM-200 spectrometer operating at 81.015 MHz and on a Bruker CXP-300 spectrometer operating at 121.442 MHz with trimethyl phosphate (TMP) in toluene-*d*₈ as an external reference. The variable-temperature ³¹P{¹H} NMR spectra of toluene-*d*₈ solutions of the sample were recorded on a Bruker AM-500 spectrometer operating at 202.462 MHz with TMP as an external reference.

The infrared (IR) spectra were measured in CsI pellets on a Perkin-Elmer 1720-X Fourier transform infrared spectrometer in the range 4000–220 cm⁻¹. Cyclic voltammetric measurements, performed with a conventional three-electrode configuration, were carried out with a Princeton Applied Research 273 potentiostat under dinitrogen atmosphere. The measurements were done in toluene-acetonitrile (1:1 v:v) with platinum working and auxiliary electrodes; the reference was a Ag/Ag⁺ (0.10 M AgNO₃) electrode in toluene-acetonitrile (1:1 v:v). Tetra-*n*-butylammonium hexafluorophosphate (0.1 M) was used as a background electrolyte. The concentration of the electrochemical active species was 2 × 10⁻⁴ M.

Preparations. [Pt(H)(PPh₃)(AuPPh₃)₇](NO₃)₂¹¹ and Ag(PPh₃)(NO₃)¹⁷ were prepared according to literature methods. All solvents were of reagent grade and were used without further purification.

[Pt₂(AuPPh₃)₁₀Ag₁₃Cl₇]. A 200-mg (0.0527-mmol) sample of [Pt(H)(PPh₃)(AuPPh₃)₇](NO₃)₂ was dissolved in 8 mL of methanol, and 91 mg (0.211 mmol) of Ag(PPh₃)(NO₃) was added. This mixture was stirred for 24 h under exclusion of light, while the color changed from red to brown. The mixture was filtered over diatomaceous earth to remove metallic contaminations. To the filtrate 10 mL of a saturated NaCl solution in methanol was added, upon which a brown precipitate was formed. This precipitate was filtered off and washed with 30 mL of methanol and 50 mL of hexane. The brown residue was then dissolved in 3 mL of toluene. After addition of 25 mL of dimethyl sulfoxide the mixture was allowed to stand for 2–4 days. In this period a dark red precipitate was formed. The mixture was filtered and the residue washed with 50 mL of methanol and 10 mL of diethyl ether. To remove minor amounts of metallic contaminations the dark red solid was dissolved in toluene and filtered over a 5-cm layer of diatomaceous earth. The red filtrate was evaporated to dryness under reduced pressure. The dark red residue was then redissolved in toluene; after slow diffusion of this toluene solution into diethyl ether, plenty of dark red diethyl ether containing crystals of [Pt₂(AuPPh₃)₁₀Ag₁₃Cl₇] were obtained, all of the same color and morphology (yield: 26 mg, 0.0039 mmol; 24% calculated for Ag). The compound is stable under normal ambient conditions; however the crystals lose the diethyl ether molecules upon exposure to air.

Anal. Calcd for Pt₂Au₁₀Ag₁₃P₁₀C₁₈₀H₁₅₀Cl₇ (*M*_r = 6633.19): C, 32.59; H, 2.28. Found: C, 32.63; H, 2.35. The infrared spectrum shows Ag–Cl stretching vibrations at 246 cm⁻¹ and several absorption bands characteristic for the PPh₃ ligands. ³¹P NMR (Figure 2A): doublet (splitting 50 Hz) at δ = 59.6 ppm with ²J(P–¹⁹⁵Pt) (doublet) ca. 520 Hz; the doublet splitting of 50 Hz and the width of the signals probably is the result of several P–Ag couplings (see Results and Discussion).

Structure Determination of [Pt₂(AuPPh₃)₁₀Ag₁₃Cl₇]. Collection and Reduction of Crystallographic Data. Since single crystals decomposed very quickly upon removal from the solvent mixture, a crystal of the compound was mounted in a capillary together with a mixture of toluene and diethyl ether. X-ray data were measured on a Nonius CAD4 diffractometer. Standard experimental details are given elsewhere.¹⁸ The crystal data are listed in Table 1. No extinction correction was performed.

Solution and Refinement of the Structure. The positions of the metal atoms were found by an orientation (ORIENT¹⁹) and a translation search (TRACOR¹⁹) with a Au₇Ag₆ fragment from [(*p*-Tol₃P)₁₀Au₁₃Ag₁₂Br₃](PF₆)₂₀ followed by a phase extension procedure (DIRDIF¹⁹). The structure was refined by full-matrix least squares using SHELX.¹⁹ The phenyl carbon atoms were obtained by rotation of an ideal phenyl

Table 1. Crystal Data for [Pt₂(AuPPh₃)₁₀Ag₁₃Cl₇]

chem formula	C ₂₂₀ H ₂₅₀ Ag ₁₃ Au ₁₀ Cl ₇ O ₁₀ P ₁₀ Pt ₂
unknown solvent	<i>n</i> C ₄ H ₁₀ O, <i>n</i> = 10 ± 2
<i>f</i> _w (<i>n</i> = 10)	7374.4
<i>a</i>	17.154(2) Å
<i>b</i>	25.256(2) Å
<i>c</i>	29.889(2) Å
β	106.12(2)°
<i>V</i>	12439 Å ³
<i>Z</i>	2
space group	<i>P</i> 2 ₁ / <i>m</i> (No. 11)
<i>T</i>	20 °C
λ	0.7107 30 Å
ρ _{calc} (<i>n</i> = 10)	1.969 g/cm ³
μ(Mo Kα) (<i>n</i> = 10)	81.59 cm ⁻¹
<i>R</i> (<i>F</i> _o) ^a	0.089
<i>R</i> _w (<i>F</i> _o) ^b	0.084

$$^a R = \sum |F_o| - |F_c| / \sum |F_o|. \quad ^b R_w = [\sum w(F_o - |F_c|)^2 / \sum w F_o^2]^{0.5}.$$

Table 2. Selected Fractional Positional and Thermal Parameters (Å²) for [Pt₂(AuPPh₃)₁₀Ag₁₃Cl₇]

atom	<i>x</i>	<i>y</i>	<i>z</i>	100 <i>U</i> _{eq} ^a
Pt	0.3624(2)	0.1376(2)	0.2262(1)	4.0(2)
Au(1)	0.2395(2)	0.0937(2)	0.1608(1)	5.3(2)
Au(2)	0.2479(2)	0.0905(2)	0.2582(1)	5.7(2)
Au(3)	0.4158(2)	0.0966(2)	0.3120(1)	6.3(2)
Au(4)	0.5112(2)	0.0948(2)	0.2463(1)	7.0(2)
Au(5)	0.4030(2)	0.0959(2)	0.1531(1)	5.8(2)
Ag(1)	0.3600(6)	0.2500	0.2265(4)	4.8(5)
Ag(2)	0.2126(4)	0.1893(3)	0.2088(2)	5.5(3)
Ag(3)	0.3236(4)	0.1902(3)	0.2992(2)	6.2(4)
Ag(4)	0.4880(4)	0.1921(4)	0.2892(3)	7.2(4)
Ag(5)	0.4755(4)	0.1915(4)	0.1911(3)	6.7(4)
Ag(6)	0.3046(4)	0.1916(3)	0.1412(2)	5.3(3)
Ag(7)	0.3674(5)	0.0254(3)	0.2265(3)	7.3(4)
Cl(1)	0.094(2)	0.2500	0.201(1)	9(2)
Cl(2)	0.289(2)	0.2500	0.358(1)	8(2)
Cl(3)	0.599(2)	0.2500	0.334(1)	7(2)
Cl(4)	0.562(2)	0.2500	0.158(2)	11(2)
Cl(5)	0.247(2)	0.2500	0.073(1)	6(2)
Cl(6)	0.374(2)	-0.064(1)	0.228(1)	11(2)
P(1)	0.137(2)	0.057(1)	0.101(1)	7(2)
P(2)	0.152(2)	0.048(1)	0.286(1)	8(2)
P(3)	0.455(2)	0.064(1)	0.386(1)	8(2)
P(4)	0.639(2)	0.060(1)	0.265(1)	10(2)
P(5)	0.441(2)	0.063(1)	0.091(1)	6(2)

$$^a U_{eq} = 1/3 \sum_i \sum_j a_i^* a_j^* a_i a_j U_{ij}.$$

group (C–C = 1.40 Å) to match maximum electron density in the difference Fourier synthesis. Their hydrogen atoms were placed at ideal positions (C–H = 1.00 Å). Each phenyl group was included in the refinement with constrained isotropic temperature factors. So far, the structural parameters describe a structure with large channels. A difference Fourier showed, among many spurious peaks, the presence of some disordered partially occupied diethyl ether molecules, while no trace of toluene-shaped fragments could be observed. Therefore we conclude that the channels are filled with disordered diethyl ether molecules (in liquid-like arrangements). The positional parameters and occupation factors of four diethyl ether molecules were refined with a constrained ideal geometry. The total occupation factor leads to slightly more than one solvent molecule per cluster, but from the spurious peaks and from an estimation of the volume of the channels it is expected that there is a total of approximately 10 diethyl ether molecules per cluster molecule. These spurious peaks were ignored during the refinement. During the final stage of the refinement, the anisotropic parameters of the gold, platinum, silver, phosphorus, and chlorine atoms were refined. Final convergence was reached at *R* = 0.089. The function minimized was $\sum w(F_o - F_c)^2$ with $w = 4.275 / [\sigma^2(F_o) + 0.0008 F_o^2]$ for 3585 reflections. The maximum shift/esd = 0.47, and the number of refined parameters is 352. A maximum residual density of 1.3 e/Å³ was found near the heavy atoms. Further residual density peaks of 0.7 e/Å³ or less are assigned to uninterpreted disordered solvent molecules.

Positional and thermal parameters of selected atoms are given in Table 2, and selected bond distances and angles in Table 3. The molecular structure of [Pt₂(AuPPh₃)₁₀Ag₁₃Cl₇] is given in Figure 1.²¹

- (16) Boyle, P. D.; Johnson, B. J.; Alexander, B. D.; Casalnuovo, J. A.; Gannon, P. R.; Johnson, S. M.; Larka, E. A.; Mueting, A. M.; Pignolet, L. H. *Inorg. Chem.* 1987, 26, 1346.
 (17) Stein, R. A.; Knobler, C. *Inorg. Chem.* 1977, 16, 242.
 (18) Smits, J. M. M.; Behm, H.; Bosman, W. P.; Beurskens, P. T. J. *Crystallogr. Spectrosc. Res.* 1988, 18, 447.
 (19) Computer references for ORIENT, TRACOR, and DIRDIF (Beurskens et al.) and SHELX (Sheldrick) are listed in ref 18.
 (20) Teo, B. K.; Zhang, H.; Shi, X. *Inorg. Chem.* 1990, 29, 2083.

Table 3. Selected Bond Lengths (Å) and Bond Angles (deg) for $[\text{Pt}_2(\text{AuPPH}_3)_{10}\text{Ag}_{13}\text{Cl}_7]$

Pt–Au(1)	2.684(5)	Au(4)–Ag(4)	2.850(9)
Pt–Au(2)	2.689(6)	Au(4)–Ag(5)	2.915(9)
Pt–Au(3)	2.679(5)	Au(5)–Ag(5)	2.807(9)
Pt–Au(4)	2.682(5)	Au(5)–Ag(6)	2.912(9)
Pt–Au(5)	2.685(6)	Au(5)–Ag(7)	3.015(9)
Pt–Ag(1)	2.839(4)	Ag(1)–Ag(2)	2.878(11)
Pt–Ag(2)	2.800(8)	Ag(1)–Ag(3)	2.854(12)
Pg–Ag(3)	2.789(9)	Ag(1)–Ag(4)	2.861(10)
Pt–Ag(4)	2.798(8)	Ag(1)–Ag(5)	2.897(13)
Pt–Ag(5)	2.801(9)	Ag(1)–Ag(6)	2.870(11)
Pt–Ag(6)	2.810(8)	Ag(2)–Ag(3)	2.842(10)
Pt–Ag(7)	2.833(9)	Ag(2)–Ag(6)	2.889(11)
Au(1)–Au(2)	2.876(5)	Ag(3)–Ag(4)	2.918(11)
Au(1)–Au(5)	2.876(5)	Ag(4)–Ag(5)	2.879(11)
Au(2)–Au(3)	2.886(5)	Ag(5)–Ag(6)	2.896(10)
Au(3)–Au(4)	2.885(6)	Ag(2)–Ag(2')	3.07(1)
Au(4)–Au(5)	2.885(5)	Ag(3)–Ag(3')	3.02(1)
Au(1)–Ag(2)	2.911(9)	Ag(4)–Ag(4')	2.93(1)
Au(1)–Ag(6)	2.840(9)	Ag(5)–Ag(5')	2.96(1)
Au(1)–Ag(7)	3.040(8)	Ag(6)–Ag(6')	2.95(1)
Au(2)–Ag(2)	2.878(9)	Ag(2)–Cl(1)	2.50(3)
Au(2)–Ag(3)	2.941(9)	Ag(3)–Cl(2)	2.52(3)
Au(2)–Ag(7)	2.980(9)	Ag(4)–Cl(3)	2.48(2)
Au(3)–Ag(3)	2.810(9)	Ag(5)–Cl(4)	2.48(3)
Au(3)–Ag(4)	2.877(9)	Ag(6)–Cl(5)	2.49(3)
Au(3)–Ag(7)	3.045(9)	Ag(7)–Cl(6)	2.27(3)
Au(4)–Ag(7)	2.947(9)		
Pt–Au(1)–P(1)	176.9(6)	Pt–Ag(5)–Cl(4)	171.7(4)
Pt–Au(2)–P(2)	178.5(8)	Pt–Ag(6)–Cl(5)	171.2(3)
Pt–Au(3)–P(3)	176.5(8)	Pt–Ag(7)–Cl(6)	178.6(9)
Pt–Au(4)–P(4)	178.4(8)	Ag(2)–Cl(1)–Ag(2')	75.7(4)
Pt–Au(5)–P(5)	177.8(7)	Ag(3)–Cl(2)–Ag(3')	73.7(4)
Pt–Ag(2)–Cl(1)	169.1(3)	Ag(4)–Cl(3)–Ag(4')	72.3(4)
Pt–Ag(3)–Cl(2)	171.6(3)	Ag(5)–Cl(4)–Ag(5')	72.7(4)
Pt–Ag(4)–Cl(3)	170.4(3)	Ag(6)–Cl(5)–Ag(6')	72.8(4)

Results and Discussion

The reaction of $[\text{Pt}(\text{H})(\text{PPh}_3)(\text{AuPPH}_3)_7](\text{NO}_3)_2$ with $\text{Ag}(\text{PPh}_3)(\text{NO}_3)$ in a molar ratio of 1:4, followed by the addition of NaCl, gives the ternary Pt–Au–Ag cluster compound $[\text{Pt}_2(\text{AuPPH}_3)_{10}\text{Ag}_{13}\text{Cl}_7]$ in 24% yield. $[\text{Pt}_2(\text{AuPPH}_3)_{10}\text{Ag}_{13}\text{Cl}_7]$ was characterized by elemental analysis, FAB-MS, cyclic voltammetry, and IR and ^{31}P NMR spectroscopy. Its solid-state structure was determined by means of a single-crystal X-ray analysis. The X-ray structure analysis of the solid shows that the cluster has a 25-metal-atom core formed by two identical icosahedral units sharing a single common vertex. The two platinum atoms are situated in the centers of these two icosahedral units as confirmed by the ^{31}P NMR spectrum (*vide infra*). Icosahedral-based structures are often found for (mixed-metal) gold cluster compounds.^{2,5,10} The cluster can be viewed as having a metal layer arrangement of 1 Ag–5 Au–1 Pt–5 Ag–1 Ag–5 Au–1 Pt–5 Au–1 Ag of D_{5h} symmetry (Figure 1). Along the C_5 axis an alternating Ag–Pt–Ag–Pt–Ag chain is formed, the central silver atom being the vertex shared by the two icosahedral units. In the 25-metal-atom supraclusters known so far, this position was occupied by a Au atom.^{12–14,22,23} The four silver and gold pentagons of $[\text{Pt}_2(\text{AuPPH}_3)_{10}\text{Ag}_{13}\text{Cl}_7]$ are ordered according to a staggered/eclipsed/staggered configuration giving rise to icosahedral coordination of the platinum atoms and a bicapped pentagonal prismatic coordination of Ag(1). Each of the gold atoms is bonded to a phosphine; Ag(7) and Ag(7') are bonded to Cl in a terminal way, whereas the two Ag pentagons are interconnected through five bridging Cl atoms (Figure 1) situated in the mirror plane perpendicular to the C_5 axis.

As in other staggered/eclipsed/staggered 25-metal-atom supraclusters^{12,13} the intraicosahedral peripheral metal–metal dis-

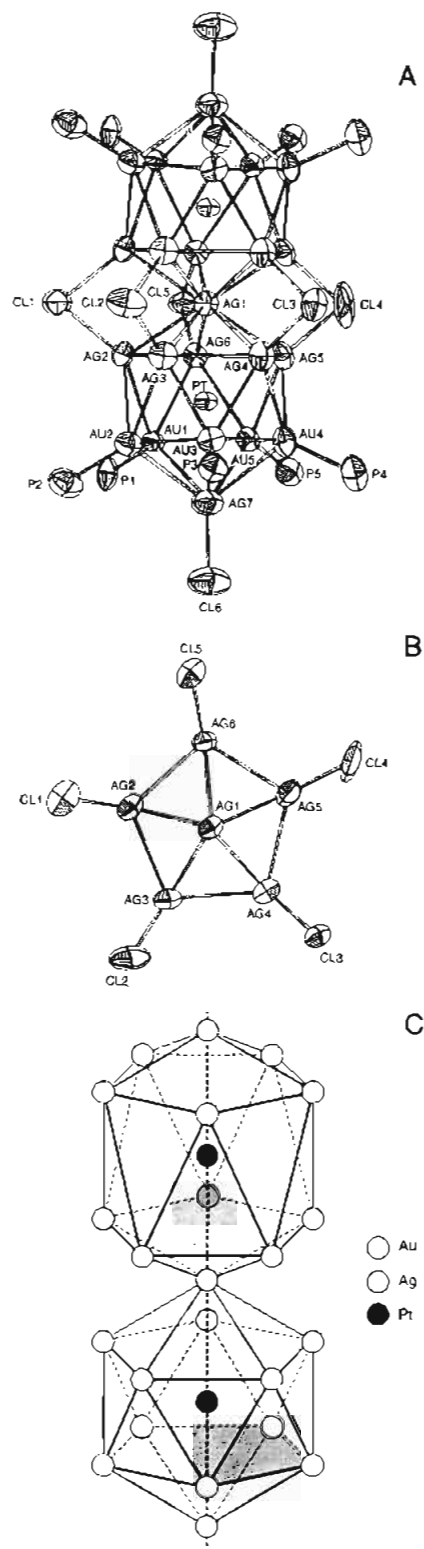


Figure 1. (A) Top: X-ray structure of $[\text{Pt}_2(\text{AuPPH}_3)_{10}\text{Ag}_{13}\text{Cl}_7]$ with atom labeling for Pt, Au, Ag, P, and Cl. Phenyl rings have been omitted for the sake of clarity. Thermal ellipsoids are at 50% probability. (B) Middle: Projection of the two silver pentagons onto the crystallographic mirror plane passing through the five doubly bridging chloride ligands and the central silver (Ag(1)). (C) Bottom: Schematic representation of the metal core of $[\text{Pt}_2(\text{AuPPH}_3)_{10}\text{Ag}_{13}\text{Cl}_7]$.

tances are significantly shorter than the intericosahedral peripheral metal–metal distances, i.e. between the silver atoms of the adjacent silver pentagons (Table 3). This observation is further support of the “cluster of clusters” concept,¹⁵ which describes this kind of supracluster as being composed of smaller building blocks, in this case the icosahedral Pt-centered subcluster units.

(21) Johnson, C. K. *A Thermal-ellipsoid Plot Program for Crystal Structures Illustrations*; Oak Ridge National Laboratory: Oak Ridge, TN, 1965.

(22) Teo, B. K.; Zhang, H. *Angew. Chem.* **1992**, *104*, 447.

(23) Teo, B. K.; Keating, K. *J. Am. Chem. Soc.* **1984**, *106*, 2224.

The radial Pt–Au distances, ranging from 2.679 to 2.689 Å, are smaller than the radial Pt–Ag distances, ranging from 2.789 to 2.839 Å. Both are in the range normally found for mixed Pt–Au–Ag clusters.⁹ The peripheral Au–Au distances range from 2.876 to 2.886 Å, and the peripheral Au–Ag distances from 2.807 to 3.045 Å; the peripheral Ag–Ag distances range from 2.842 to 2.918 Å for intraicosahedral distances, whereas the intericosahedral Ag–Ag distances range from 2.93 to 3.07 Å. The Pt–Ag(7)–Cl(6) bond angle (178.6°) slightly deviates from linearity.

The central Pt atoms are surrounded in a spheroidal geometry which is in accordance with the $(S^{\sigma})^2(P^{\sigma})^6$ electron configuration (18 electrons) of the Pt-centered subclusters of this supracluster.^{24,25} The observation that this electron counting principle still holds for these subclusters can be seen as further support of the “cluster of clusters” concept.

The cluster compound $[\text{Pt}_2(\text{AuPPH}_3)_{10}\text{Ag}_{13}\text{Cl}_7]$ also satisfies the electron counting rule developed by Teo on the basis of the Hume–Rothery rule.²⁶ This rule predicts a total of 310 valence electrons for a close-packed high-nuclearity cluster with 3 encapsulated (“bulk”) and 22 peripheral (“surface”) metal atoms arranged in a pentagonal geometry. The observed number of valence electrons is 2×10 (Pt) + 10×11 (Au) + 10×2 (PPH₃) + 13×11 (Ag) + 5×3 (bridging Cl) + 2×1 (terminal Cl) = 310. This electron counting therefore supports the premise that no hydrogen atoms are bonded to the central Pt atoms (which is the case for the starting cluster $[\text{Pt}(\text{H})(\text{PPH}_3)(\text{AuPPH}_3)_7](\text{NO}_3)_2$), which is in accordance with the absence of ¹H NMR signals originating from Pt-bonded hydrogen atoms.²⁷ The impossibility to exchange counterions and the solubility in benzene and toluene show this $[\text{Pt}_2(\text{AuPPH}_3)_{10}\text{Ag}_{13}\text{Cl}_7]$ cluster to be a neutral molecule.

The ³¹P NMR spectrum of $[\text{Pt}_2(\text{AuPPH}_3)_{10}\text{Ag}_{13}\text{Cl}_7]$ consists of a doublet signal at $\delta = 59.6$ ppm with Pt satellites with $^2J(\text{P}^{195}\text{Pt})$ (doublet) of approximately 520 Hz. This NMR appearance, together with the intensity of the Pt satellites, unambiguously proves that the platinum atoms are situated in the centers of both icosahedral subclusters, surrounded by AuPPH₃ groups, as the magnitude of $J(\text{P}^{195}\text{Pt})$ is in the range normally found for 2J -couplings via a gold nucleus.^{11,28} Because the 10 AuPPH₃ groups are symmetry related, only one δ -value is observed. The 4J -coupling between the PPH₃ ligands on one icosahedral subcluster, and the Pt atom on the other icosahedral subunit probably is too small to be observed. The doublet splitting of 50 Hz of the ³¹P NMR signal (Figure 2A) is an indication of the presence of one unique Ag atom, which is confirmed by the X-ray analysis as described above (Figure 1; Ag(1)).

This observed ³¹P NMR spectrum can be perfectly matched by simulation (Figure 2B²⁹) assuming that $^3J(\text{P}^{109}\text{Ag})$ of the five Ag atoms from the Ag pentagon is approximately 13 Hz (assuming $^4J(\text{P}^{109}\text{Ag})$ of the adjacent Ag pentagon is too small to give any effect), that $^3J(\text{P}^{109}\text{Ag})$ of the top (or bottom) peripheral Ag atom (Ag(7) or Ag(7)') amounts circa 21 Hz, and that $^3J(\text{P}^{109}\text{Ag})$ of the unique, encapsulated, Ag atom is approximately 55 Hz (the J -couplings of the ¹⁰⁷Ag isotopes are related to the J -couplings of the ¹⁰⁹Ag isotopes in accordance with the gyromagnetic ratio). The 3J -couplings of the peripheral

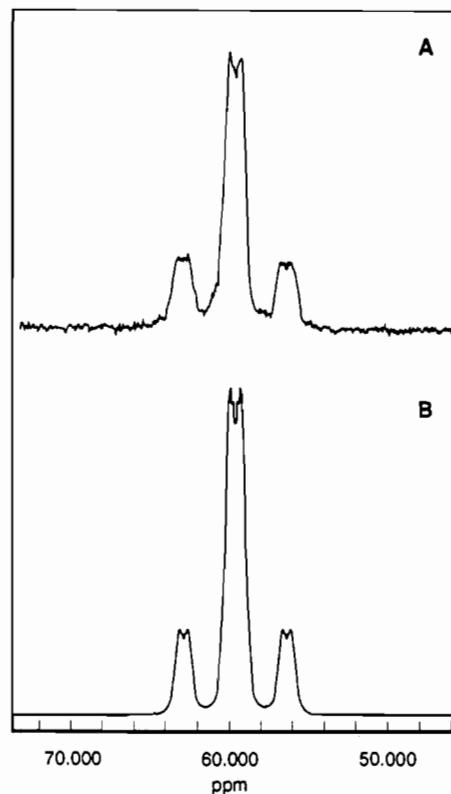


Figure 2. (A) ³¹P NMR spectrum (81.015 MHz) at 298 K for a toluene solution of $[\text{Pt}_2(\text{AuPPH}_3)_{10}\text{Ag}_{13}\text{Cl}_7]$. (B) Simulated ³¹P NMR spectrum of $[\text{Pt}_2(\text{AuPPH}_3)_{10}\text{Ag}_{13}\text{Cl}_7]$. (See Results and Discussion.)

Ag atoms are in the range normally found for peripheral Ag atoms in mixed Pt–Au–Ag cluster compounds.^{9,30}

In this simulation the J -coupling of the unique central Ag atom (circa 55 Hz) largely accounts for the doubletlike splitting pattern of approximately 50 Hz; furthermore the equivalence of the PPH₃ ligands, together with that of the five Ag atoms in one pentagon, assumes a fast fluxional behavior in solution which is commonly observed for mixed-metal gold phosphine cluster compounds.³⁰ This fast fluxionality may include rotation of the AuPPH₃ groups or PPH₃ ligands with regard to the adjacent Ag pentagon.

The ³¹P NMR spectrum, as described, does not change in the temperature range 298–193 K. These NMR data and the observed neutrality of the cluster molecule show that both icosahedra are centered by Pt atoms; this in contrast with the recently published cluster compound $[\text{PtAu}_2(\text{AuPPH}_3)_{10}\text{Ag}_{12}\text{Cl}_7]\text{Cl}$,³¹ which is isomorphous and isostructural to the title compound.

The IR spectrum of $[\text{Pt}_2(\text{AuPPH}_3)_{10}\text{Ag}_{13}\text{Cl}_7]$ (Figure 3) shows an absorption at 246 cm⁻¹ which can be attributed to a Ag–Cl vibration. This assignment is in agreement with the observation of the metal–halide absorptions in other compounds.^{6,32} Furthermore only a absorption bands characteristic for the PPH₃ ligands were observed.

The molecular composition of $[\text{Pt}_2(\text{AuPPH}_3)_{10}\text{Ag}_{13}\text{Cl}_7]$ was also confirmed by FAB-MS. This technique has been shown to be successful for the determination of the correct molecular composition of cationic clusters.¹⁶ The positive ion FAB-MS in the 4500–7000 mass range has a large number of peaks (Figure 4). A selection of the centroids of heavy fragments as well as their assignments is given in Table 4. The result is in good agreement with the composition and the structure of the cluster as discussed above. Some peaks with masses higher than that of

(24) Kanters, R. P. F.; Steggerda, J. J. *J. Cluster Sci.* **1990**, *1*, 229.

(25) Mingos, D. M. P.; Kanters, R. P. F. *J. Organomet. Chem.* **1990**, *384*, 405.

(26) Teo, B. K. *J. Chem. Soc., Chem. Commun.* **1983**, 1362.

(27) Kappen, T. G. M. M.; Bour, J. J.; Schlebos, P. P. J.; Roelofsens, A. M.; van der Linden, J. G. M.; Steggerda, J. J.; Aubart, M. A.; Krogstad, D. A.; Schoondergang, M. F. J.; Pignolet, L. H. *Inorg. Chem.* **1993**, *32*, 1074. Bour, J. J.; Schlebos, P. P. J.; Kanters, R. P. F.; Schoondergang, M. F. J.; Addens, H.; Overweg, A.; Steggerda, J. J. *Inorg. Chim. Acta* **1991**, *181*, 195.

(28) Bour, J. J.; Kanters, R. P. F.; Schlebos, P. P. J.; Steggerda, J. J. *Recl. Trav. Chim. Pays-Bas* **1988**, *107*, 211.

(29) Budzelaar, P. H. M. *geNMR, NMR Simulation Program V3.4*; IvorySoft: Amsterdam, 1992.

(30) Kanters, R. P. F.; Schlebos, P. P. J.; Bour, J. J.; Steggerda, J. J.; Maas, W. E. J. R.; Janssen, R. *Inorg. Chem.* **1991**, *30*, 1709.

(31) Teo, B. K.; Zhang, H.; Shi, X. *J. Am. Chem. Soc.* **1993**, *115*, 8489.

(32) Teo, B. K.; Barnes, D. M. *Inorg. Nucl. Chem. Lett.* **1976**, *12*, 681.

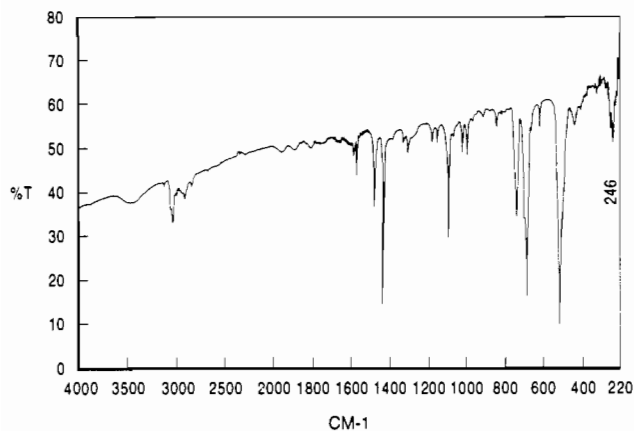


Figure 3. IR spectrum of $[\text{Pt}_2(\text{AuPPh}_3)_{10}\text{Ag}_{13}\text{Cl}_7]$ (CsI pellet). The Ag–Cl stretching vibration is labeled with its wavenumber; other bands originate from the PPh_3 ligands.

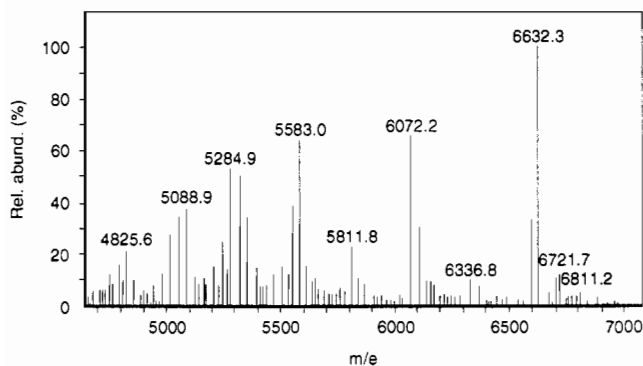


Figure 4. Low resolution positive ion FAB-MS spectrum of $[\text{Pt}_2(\text{AuPPh}_3)_{10}\text{Ag}_{13}\text{Cl}_7]$ in the m/e 4500–7000 mass range.

Table 4. Positive Ion FAB-MS Data for $[\text{Pt}_2(\text{AuPPh}_3)_{10}\text{Ag}_{13}\text{Cl}_7]$ ($M = \text{Pt}_2\text{Au}_{10}(\text{PPh}_3)_{10}\text{Ag}_{13}\text{Cl}_7$)

rel mass, ^a m/e	% abundance	assgnt
6632.3	100	M^+
6597.4	32	$(M - \text{Cl})^+$
6072.2	66	$(M - 2\text{PPh}_3 - \text{Cl})^+$
5811.8	22	$(M - 3\text{PPh}_3 - \text{Cl})^+$
5583.0	63	$(M - 4\text{PPh}_3)^+$
5284.9	52	$(M - 2\text{Au} - 2\text{PPh}_3 - 3\text{Ag} - 3\text{Cl})^+$

^a Not matched.

M^+ are observed; however, the relative abundances of these peaks are not significant, i.e. about 10% or less. Two of these peaks, however, may be assigned to the compositions $\text{Pt}_2\text{Au}_{11}\text{Ag}_{12}(\text{PPh}_3)_{10}\text{Cl}_7$ (theoretically at m/e 6722.3; observed at m/e 6721.7, with relative abundance 12%) and $\text{Pt}_2\text{Au}_{12}\text{Ag}_{11}(\text{PPh}_3)_{10}\text{Cl}_7$ (theoretically m/e at 6811.4; observed m/e at 6811.2, with relative abundance 5%), respectively. These peaks originate either from recombination products formed in the FAB-MS experiment or from minor contaminations of other cluster compounds in the

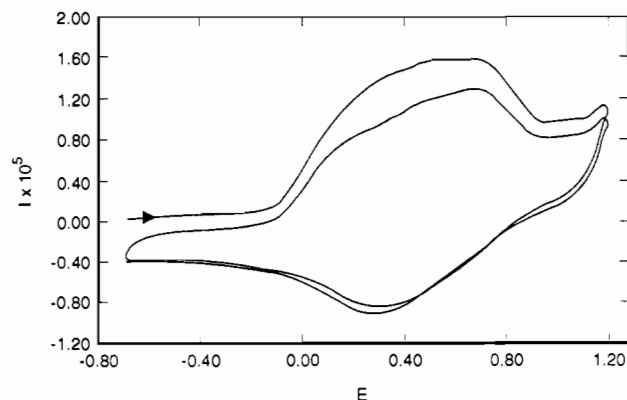


Figure 5. Cyclic voltammogram of a toluene–acetonitrile (1:1 v:v) solution of $[\text{Pt}_2(\text{AuPPh}_3)_{10}\text{Ag}_{13}\text{Cl}_7]$ (vs Ag/Ag^+ (0.10 M AgNO_3) reference electrode; scan rate 500 mV/s).

sample. These contaminations might be analogous to $[\text{Pt}_2(\text{AuPPh}_3)_{10}\text{Ag}_{13}\text{Cl}_7]$ with the terminal Ag–Cl groups replaced by one or two Au–Cl groups, respectively: $[\text{Pt}_2(\text{AuPPh}_3)_{10}\text{Ag}_{12}\text{AuCl}_7]$ and $[\text{Pt}_2(\text{AuPPh}_3)_{10}\text{Ag}_{11}\text{Au}_2\text{Cl}_7]$.

Cyclic voltammetric studies of $[\text{Pt}_2(\text{AuPPh}_3)_{10}\text{Ag}_{13}\text{Cl}_7]$ show a broad irreversible oxidation from -0.15V to $+0.90\text{V}$. At a scan rate of 500 mV/s at least three separate oxidative steps can be observed (Figure 5). At higher scan rates the cyclic voltammogram qualitatively remains the same, but the separate steps blend into each other. The width of the oxidative area (1.05 V) is indicative of a multi-electron redox process.³³ This electrochemical behavior is in agreement with the electron counting as mentioned above: the two spheroidal 18-electron Pt-centered icosahedral subclusters of $[\text{Pt}_2(\text{AuPPh}_3)_{10}\text{Ag}_{13}\text{Cl}_7]$ can theoretically be oxidized to 16-electron systems. Such 16-electron systems should adopt a toroidal geometry,²⁴ but this is certainly inhibited because of steric hindrance. Oxidation of $[\text{Pt}_2(\text{AuPPh}_3)_{10}\text{Ag}_{13}\text{Cl}_7]$ will therefore lead to (partial) decomposition, which is revealed in the irreversible nature of the oxidation process.

Acknowledgment. This investigation was supported by the Netherlands Foundation for Chemical Research (SON) with fundamental support from the Netherlands Organization for the Advancement of Pure Research (NWO). We acknowledge Mrs. Annie Roelofsen and Dr. J. G. M. van der Linden for the electrochemical measurements and the contributions of Mr. Henk Husken and Mr. Marcel van der Woude. Prof. L. H. Pignolet is gratefully thanked for his fruitful discussions and for providing us the opportunity to do FAB-MS experiments.

Supplementary Material Available: Tables of crystallographic details, additional fractional positional and thermal parameters, anisotropic thermal parameters, and bond distances and angles (9 pages). Ordering information is given on any current masthead page.

(33) Steggerda, J. J.; van der Linden, J. G. M.; Gootzen, J. E. F. *Mater. Res. Soc. Symp. Proc.* **1992**, 272, 127.